Digital hologram as a display optical system

Dyomin, Victor, Davydova, Alexandra, Polovtsev, Igor, Olshukov, Alexey

Victor Dyomin, Alexandra Davydova, Igor Polovtsev, Alexey Olshukov, "Digital hologram as a display optical system," Proc. SPIE 11710, Practical Holography XXXV: Displays, Materials, and Applications, 117100B (5 March 2021); doi: 10.1117/12.2577727

SPIE.

Event: SPIE OPTO, 2021, Online Only

Digital hologram as a display optical system

Victor Dyomin[a], Alexandra Davydova*[a,b], Igor Polovtsev[a], Alexey Olshukov[a,b]
[a]National Research Tomsk State University, 36 Lenin Avenue, Tomsk, Russia, 634050; [b]V.E. Zuev Institute of Atmospheric Optics SB RAS, 1 Academician Zuev Square, Tomsk, Russia, 634055

ABSTRACT

The holographic system is usually used for imaging, so it can be attributed to imaging optical systems. This analogy allows using a well-developed computational optics technique to design and analyze real digital holographic systems, as well as to solve the measuring tasks of digital holography. The work presents a mathematical model that establishes a one-to-one correspondence between dimensional and spatial parameters of a digital holographic image and a holographing object for the given case of an in-line scheme. The values of the model constants used to determine the real size and the longitudinal coordinate of an object according to its holographic image are found through calibration. The described approach is used to calibrate and analyze the imaging properties of a submersible digital holographic camera designed to study plankton in its habitat. The paper also shows the results obtained in situ using the holographic sensor of plankton.

Keywords: digital holographic system, equivalent optical scheme, calibration, holographic sensor for plankton study, submersible digital camera

1. INTRODUCTION

The methods of digital holography of particles are widely used in measuring tasks, for example, to study plankton [1-8], microplastics [9-10], bubbles [11-13], aerosol particles [14-17], defects in optical crystals [1, 18]. Most commonly, an in-line scheme is used for this purpose when the studied volume with particles is illuminated with coherent monochromatic radiation, and a CCD camera is placed in the area of interference of light passing by the particles (reference wave) and light diffracted on the particles (object wave). The interference pattern thus recorded represents a digital hologram and contains information on the size, shape and spatial coordinates of each particle. The particle images are reconstructed numerically by calculating the diffraction integral [19-23]. It is possible to determine geometric and spatial characteristics according to the reconstructed images of particles.

The classical in-line lensless digital holography scheme assumes that the reconstructed images are identical to the particles themselves. Therefore, the characteristics of a reconstructed image relate to an object and the measuring task seems solved. However, such a conclusion requires a priori information that is not always available. For example, the curvature of the illuminating wave front or the location of an equivalent point illuminating source during recording to ensure its identical simulation during the reconstruction of holographic images, or the refractive index of the medium in which the holographic object is located [13, 24].

The situation with the use of the objective lens in the object beam is even more complicated, since the holographic experiment records the image formed by this objective lens, and the curvature of the illuminating wave front in the used in-line scheme also depends on the properties of the objective lens. In this case the correlation of dimensional and spatial characteristics of the holographic image and the object becomes even more complicated as there is no reliable data on the optical characteristics of the holographic scheme with a lens, such as the focal length, focal (working) segment, refractive index of the object-side medium and the volume of hologram recording and image reconstruction.

In holography under stationary laboratory conditions such constants can be determined and the task of measuring the real sizes and coordinates of the particles under study may reach its viable solution. Under natural conditions, for example, when recording submersible holograms of particles of various origins (plankton, gas bubbles, settling particles, etc.) from the board side in the open ocean [25], similar definitions of constants and measurements of real geometric parameters of particles are quite difficult.

*starinshikova@mail.ru

Practical Holography XXXV: Displays, Materials, and Applications, edited by Hans I. Bjelkhagen, Seung-Hyun Lee, Proc. of SPIE Vol. 11710, 117100B · © 2021 SPIE
CCC code: 0277-786X/21/$21 · doi: 10.1117/12.2577727

This paper proposes to solve these problems by considering an equivalent optical scheme of an in-line digital holographic system and constructing a mathematical model using a well-developed computational optics technique. This approach is used to calibrate and analyze the image properties of a submersible digital holographic camera (DHC – Digital Holographic Camera) designed to study plankton in its habitat [25].

2. DHC EQUIVALENT OPTICAL SYSTEM

For this description, we use the generalized equivalent scheme of a digital holographic camera (DHC) shown in Figure 1. According to this scheme, the imaging in such a system includes two stages. At the first real stage, the imaging lens (1) constructs a real image, which is considered virtual with respect to the matrix receiver (2). It is appropriate to recall that the digital hologram represents a two-dimensional array of discrete quantized value of the intensity distribution of the interference pattern of the reference and object waves recorded on the matrix receiver. The second, fully virtual stage is ensured by numerical reconstruction of an image from a digital hologram [19, 21-23]. Thus, the equivalent imaging optical system (5) of the digital holographic camera is two-stage. The main parameters of this system, i.e. the equivalent focal length, decentering and magnification are determined in the general case by a set of factors: characteristics of the lens (1), position of the receiver (2), radius of curvature of the reference beam R_1, its angle of incidence θ_1, radiation wavelength λ_1 at the recording stage, radius of curvature of the virtual reconstruction beam R_2, its angle of incidence θ_2 and its wavelength λ_2. In general, the values of the angles θ_1 and θ_2 at the recording and reconstruction stages may not match. But in the most common in-line scheme in the holography of particles that we use in our works (Figure 2), they coincide and equal zero. Further, let us specifically consider the case of the in-line holographic scheme for recording particles of various nature in various media.

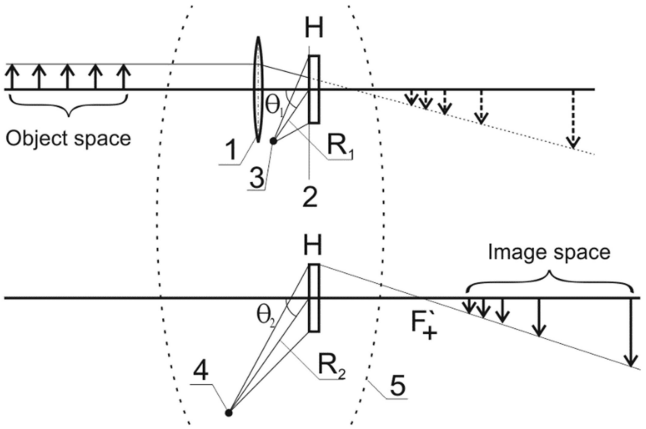

Figure 1. Optical scheme of the imaging system equivalent to a digital holographic camera designed for measuring purposes. 1 – lens forming an object image, 2 – CCD (CMOS) matrix plane used for digital hologram (H) recording, 3 – reference beam with the radius of curvature R_1 for hologram recording, 4 – simulated beam with the radius of curvature R_2 for numerical reconstruction of images from a digital hologram (H), 5 – equivalent optical system of a digital holographic camera with focal length F'_+.

The main task of the digital holographic measuring system is reliable knowledge on the size of the object under study and its location in the space of objects. This requires a mathematical model that establishes a one-to-one correspondence between a digital holographic image and a holographing (displaying) object. For this model it is necessary to determine the above factors as accurately as possible.

Due to the fact that the projection lens 1 (Figure 1) takes part in the formation of the digital hologram of particles, the magnification of this lens should affect the size and position of particle images reconstructed from the digital hologram. Let us consider Figure 2. Usually, when the Newton's formula [26-29] is derived, it is assumed that the segments in the space of objects x and in the space of images x' are counted from the front and back focal planes, the positions of focuses are indicated in Figure 2, respectively: front F and back F'. Since the position of the focus is not always known

in the optical experiment, as well as the values of the front f and back f' focal lengths of the optical system, let us write the formal formulas of the ideal optical system for the case of arbitrary coordinates, both in object and image spaces.

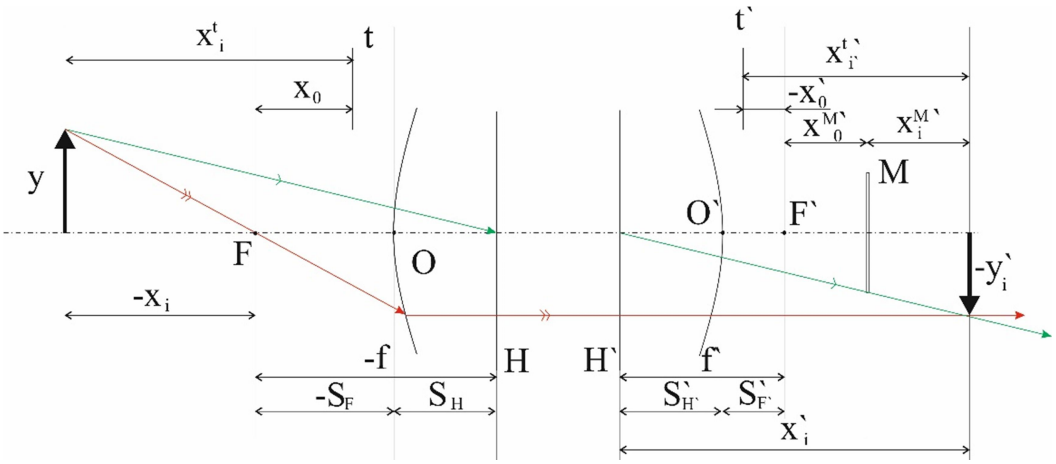

Figure 2. On the Newton's formula in an arbitrary coordinate system. H, H′ – front and back main planes of the optical system, F, F′ – front and back foci of the optical system, $S_F, S'_{F'}$ – front and back focal segments, O, O′ – tops of the first and last optical surface, $S_H, S'_{H'}$ – segments setting the position of the main planes in relation to O, O′ respectively, t and t' – arbitrary planes in the space of objects and images, respectively, relative to which the positions of objects and images are counted, M – plane of the matrix position of the digital holographic camera.

In Figure 2, the position of the reference plane t in the object space is set by the segment x_0 set from the front focal plane (plane perpendicular to the optical axis and passing through the front focus F). In the image space, the position of the reference plane t' is determined by the segment x'_0 set from the back focal plane (plane perpendicular to the optical axis and passing through the back focus F'). Let us place the recording matrix of the digital holographic camera in the plane M located at a distance x'^M_0 from the back focus F'. Here we don't take into account the details related to the conditions of such recording and the adjustment of dimensions of the matrix and the field of view in the object space. The position of reference planes t and t' for segments counting in the DHC is selected as follows: t coincides with the outer surface of the receiver porthole, t'– with the surface of the recording matrix M.

Let the i object with the size y_i in the object space be given by the segment x^t_i. Then for the segment x_i that sets the position of this object relative to the front focus we can write the relation obvious from Figure 2:

$$x_i = x^t_i - x_0. \quad (1)$$

Similar relationship is applicable for the image space:

$$x'_i = x'^{t'}_i - x'_0 \quad (2)$$

this is a segment setting the position of the image plane of the i object relative to the back focal plane, while $x^{t'}_i$ – a segment setting the position of this image relative to the plane t'. The size of this image $y'_i = \beta_i \cdot y_i$ by determining the magnification β_i of the optical system.

According to the Newton's formula, we can write:

$$x_i \cdot x'_i = f \cdot f', \quad (3)$$

moreover, in the general case $f \neq -f'$ since the object space may have different medium (water) and different optical system (a porthole and prism systems).

For magnification, taking into account (1) we get:

$$\beta_i = -\frac{f}{x_i} = -\frac{f}{x_i^t - x_0}\ , \tag{4}$$

and taking into account (2):

$$\beta_i = -\frac{x'_i}{f'} = -\frac{x'^{t'}_i - x'_0}{f'}. \tag{5}$$

By substituting the relations (1) and (2) into (3), we get the Newton's formula at random positions of the planes t and t' indicating the reference point (origins of coordinates) in object and image spaces:

$$(x_i^t - x_0) \cdot (x'^{t'}_i - x'_0) = f \cdot f'\ . \tag{6}$$

The relations (4), (5) and (6) may be used to calibrate the considered optical system (equivalent to a digital holographic measuring system).

Let us choose four different positions for objects in the object space set by the segments $x_1^t,\ x_2^t,\ x_3^t,\ x_4^t$ from the random position of the reference point t. If the dimensions of the objects are $y_1,\ y_2,\ y_3,\ y_4$, then the optical magnification for these objects will be $\beta_1,\ \beta_2,\ \beta_3,\ \beta_4$, respectively. If the hologram of the object space volume is written on a matrix, then at reconstruction we determine the sizes of images $y'_1,\ y'_2,\ y'_3,\ y'_4$ and distances from a reference point t' $x'^{t'}_1,\ x'^{t'}_2,\ x'^{t'}_3,\ x'^{t'}_4$. Using the determination of magnification, let us calculate $\beta_1,\ \beta_2,\ \beta_3,\ \beta_4$ according to given $y_1,\ y_2,\ y_3,\ y_4$ and measured $y'_1,\ y'_2,\ y'_3,\ y'_4$.

For the lens, we do not know f and f', for the reference planes t and t' are the segments x_0 and x'_0. Using the relation (4) for the first and second objects, we get the system of equations

$$\begin{cases} x_0 - x_1^t = \frac{f}{\beta_1} \\ x_0 - x_2^t = \frac{f}{\beta_2} \end{cases}.$$

By solving it in relation to unknown f and x_0, we get the corresponding formulas to determine them:

$$f = \frac{(x_1^t - x_2^t)}{\left(\frac{1}{\beta_2} - \frac{1}{\beta_1}\right)}, \tag{7}$$

$$x_0 = \frac{f \cdot \left(\frac{1}{\beta_2} + \frac{1}{\beta_1}\right) + x_1^t + x_2^t}{2}. \tag{8}$$

Then, let us write a similar system for the image space using the relation (5):

$$\begin{cases} x'_0 - x'^{t'}_3 = f' \cdot \beta_3 \\ x'_0 - x'^{t'}_4 = f' \cdot \beta_4 \end{cases}.$$

By solving it in relation to unknown f' and x'_0, we get

$$f' = \frac{x'^{t'}_3 - x'^{t'}_4}{\beta_4 - \beta_3}. \tag{9}$$

$$x'_0 = \frac{f'(\beta_3 + \beta_4) + x'^{t'}_3 + x'^{t'}_4}{2}. \tag{10}$$

Having thus determined the values of the Newton's formula constants for the random reference of the position of an object and its image $f,\ f', x_0, x'_0$ from (7), (8), (9) and (10), we can write the following for the size of an arbitrary object

$$y_i = \frac{y'_i}{\beta_i} = -\frac{y'_i \cdot f'}{x'^{t'}_i - x'_0}, \tag{11}$$

and for its position

$$x_i^t = \frac{f \cdot f'}{x'^{t'}_i - x'_0} + x_0\ . \tag{12}$$

The relations (11) and (12) are universally applicable and can be used for various purposes of digital holographic systems.

If we neglect the problem of determining the position of cardinal points and the segments of the optical system, then the simplest method of calibration is the interpolation of dependencies

$$x^t = x^t(x'^{t\prime}) \text{ и } \beta = \beta(x'^{t'}). \quad (13)$$

The exact view of the interpolation polynomial from (12) to describe the dependency $x^t(x'^{t\prime})$ is written as follows:

$$x^t = \mathrm{A} + \frac{B}{x'^{t\prime} - C}. \quad (16)$$

The exact kind of polynomial to describe the dependency $\beta\left(x'^{t'}\right)$ follows from the formula (11):

$$\beta = -\frac{x'^{t\prime} - C}{D}. \quad (17)$$

where the coefficients A, B, C, D – values having an optical interpretation. $\mathrm{A} = x_0$ – a segment set from the front focal plane, which specifies the position of the reference point in the object space (plane t). $B = f \cdot f'$ – product of the front f and back f' focal lengths of the optical system. $C = x'_0$ – a segment set from the back focal plane, which specifies the reference position in the image space (plane t'). $D = f'$ – value of the back focal length of the optical system.

In general, in a real holographic experiment, for various reasons, the wave front shape (beam convergence) does not coincide at the hologram recording stage and at the image reconstruction stage. This means that the digital hologram at the image reconstruction stage will play the role of another optical system with optical properties that depend on the divergence mismatch of the recording and reconstruction beams. As a result of the composition of two optical systems, a new optical system is formed with characteristics determined by optical forces of used components and the distance between them [29]. Therefore, the relations (16) and (17) may also be applied to this equivalent optical system. Thus, when determining the coefficients A, B, C, D from a digital holographic experiment, the difference in the shape of recording and reconstruction beams will be automatically taken into account. This is important, since when using a lens (for example, in the DHC), a converging reference beam with unknown convergence is used during recording, while the flat one is used in numerical reproduction for ease of calculation.

The problem of finding coefficients is solved by calibration in both laboratory and real conditions. For calibration, we use test particles (Figure 3) in the form of opaque squares with a side of 500 μm, placed photolithographically on a glass plate with a thickness of 2.65 mm (calibers). The DHC design provides the fixation of four calibers (Figure 4).

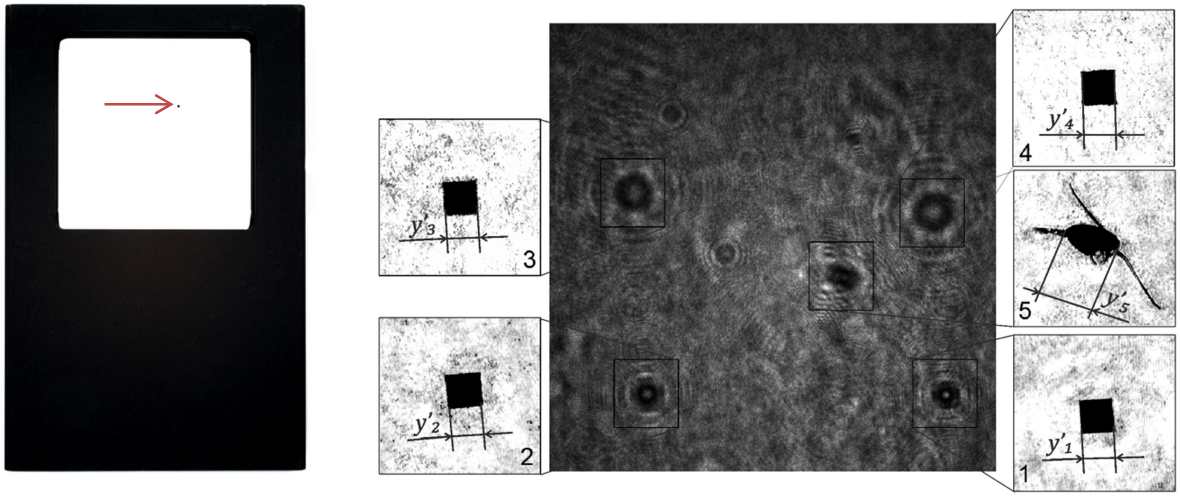

(a) (b)

Figure 3. (a) Caliber: a test particle placed on a glass plate (indicated by an arrow) in the design. (b) Digital hologram of four calibers recorded at the station No. 6939 and their holographic images. 1-4 – images of test particles of four calibers reconstructed from one hologram, 5 – images of the plankton particle reconstructed from the same hologram.

Since the refractive indices of the medium where the test particles (fresh water, sea water or air) are located differ from the refractive index of the glass, it is necessary to take into account the refractive index of the medium n_{wg} relative to the glass of calibers and prisms. Then,

$$x^t = x_w^t - x_g^t(n_{gw} - 1), \tag{18}$$

where x_w^t – geometric coordinate of the particle in the medium (design factor), x_g^t – thickness of the optical elements of the working volume. Let us define n_{gw} with E coefficient, then the expression (16) looks as follows:

$$x_w^t - x_g^t(E - 1) = \mathrm{A} + \frac{B}{x'^{t\prime} - C}. \tag{19}$$

Thus, in order to obtain the values A, B, C, D, E for the considered digital holographic system, it is necessary to solve the system of equations:

$$\begin{cases} {x_1}_w^t - {x_1}_g^t(E - 1) = \mathrm{A} + \frac{B}{{x_1}'^{t\prime} - C} \\ {x_2}_w^t - {x_2}_g^t(E - 1) = \mathrm{A} + \frac{B}{{x_2}'^{t\prime} - C} \\ {x_3}_w^t - {x_3}_g^t(E - 1) = \mathrm{A} + \frac{B}{{x_3}'^{t\prime} - C} \\ {x_4}_w^t - {x_4}_g^t(E - 1) = \mathrm{A} + \frac{B}{{x_4}'^{t\prime} - C} \\ y_1 = -\frac{{y'}_1 \cdot D}{x'^{t\prime}_1 - C} \end{cases}. \tag{20}$$

The system (20) contains 5 nonlinear equations, of which the first four can be solved by a numerical method thus finding a solution for independent coefficients A, B, C, E. The last equation in (20) allows defining the coefficient D by substituting the found values in the expression, and without the need for a fifth caliber, just simply using the measured values for the first caliber. Thus, the optimal number of calibration experiments is 4, and they can be fulfilled by simultaneous recording of four calibers per one hologram. Such calibration requires no reliable knowledge on the optical properties of components and media (in this case, water, glass and air) included in the equivalent optical scheme.

In the present work, the calibration was carried out during the field experiment of plankton study using a digital holographic camera as part of the Arctic expedition in October 2020. The digital holograms of calibers (a square of $y_1 = 500$ μm on side) were registered by submerging on two stations – No. 6935 (74°22'57.2"N 72°53'04.3"E) in the Kara Sea (Ob River estuary) on October 2 and No. 6939 (77°17'04.4"N 122°05'44.7"E) in the Laptev Sea. The positions of the best focus planes of caliber images $x'^{t\prime}_1 = x_1^{M\prime}$, $x'^{t\prime}_2 = x_2^{M\prime}$, $x'^{t\prime}_3 = x_3^{M\prime}$, $x'^{t\prime}_4 = x_4^{M\prime}$ in relation to the position of a matrix and the size (square side) of a caliber ${y'}_1$ were determined from the reconstructed images of calibers (Table 1).

For the considered DHC, the following values are known: ${x_1}_w^t = r_1 = 57.5$ mm, ${x_1}_g^t = 0$, ${x_2}_w^t = r_1 + d + r_2 = 180.65$ mm, ${x_2}_g^t = d = 2.65$ mm, ${x_3}_w^t = r_1 + 2d + r_2 + 2r_3 + 3l + 2r_4 = 816.3$ mm, ${x_3}_g^t = 2d + 3l = 305.3$ mm, ${x_4}_w^t = r_1 + 3d + 2r_2 + 2r_3 + 3l + 2r_4 = 921.45$ mm, ${x_4}_g^t = 3d + 3l = 307.95$ mm, defined at the design stage. They are shown in Figure 4.

To solve the system of nonlinear equations (20), the Levenberg-Marquardt algorithm [30, 31] is applied. The results are shown in Table 1.

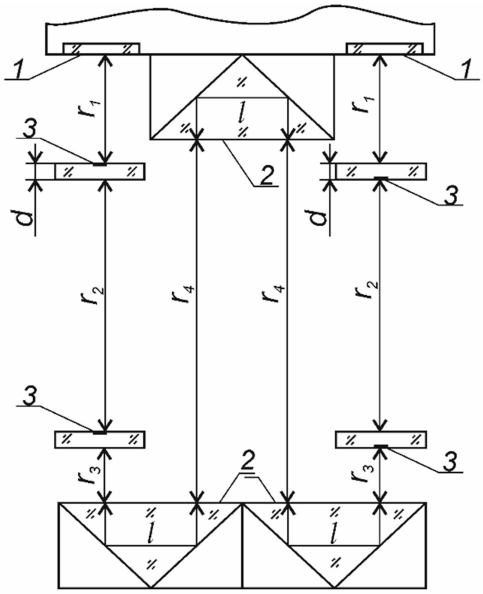

Figure 4. Scheme of the working volume of the digital holographic camera. 1 – portholes, 2 – prisms, 3 – calibers (test objects placed on a glass plate).

Table 1. DHC calibration results under different conditions.

Station	No. 6935, Kara Sea, 2 October 2020)	No. 6939, Laptev Sea, 6 October 2020)
$x_1^{M\prime}$, mm	52.4	52.4
$x_2^{M\prime}$, mm	72.2	72.9
$x_3^{M\prime}$, mm	168.05	170.05
$x_4^{M\prime}$, mm	187.25	189.91
y'_1, μm	241.5	241.5
A	-46765	-44537
B	-354206934	-333016226
C	7617	7519
D	15661	15661
E	1.1044	1.1472

Thus, using the obtained coefficients A, B, C, D, expressions (16) and (17) and data (coordinates and size) obtained from reconstructed holographic images of particles it is possible to determine the true coordinates of the particle and its size.

Figure 3 (b) shows the digital caliber hologram recorded at the station No. 6939 (Laptev Sea) at a depth of 23.8 m and the reconstructed images of test caliber particles and a plankton particle. The size of particles without any consideration given to the coefficients A, B, C, D are determined by counting the number of pixels and multiplying by the pixel size of the digital camera used (3.5 μm). The correction of dimensions taking into account the coefficients A, B, C, D from Table 1 for this station is made according to formula $y_i = -\frac{y'_i \cdot D}{x_i^{M\prime} - C}$ and is presented in Table 2. Thus, the measured size of test caliber particles taking into account the correction factors is equal to 500±8 μm.

Table 2. Size of particles, which reconstructed images are shown in Figure 3 (b), determined without taking into account coefficients A, B, C, D (y'_i) and corrected with respect to coefficients A, B, C, D from Table 1 (y_i).

For i particle in Fig. 3	1st caliber	2nd caliber	3rd caliber	4th caliber	5 - plankton particle
y'_i, μm	241.5	238	234.5	231	388.5
y_i, μm	506.54	500.57	499.73	493.60	815.64

It shall be noted that the coefficients A, B, C, D characterize the optical system of the DHC camera automatically taking into account the medium in which the holograms are recorded.

Besides, the obtained results show that the E coefficient for the two stations differs by ~ 3.9%, which means that the refractive index of water in the Kara Sea and in the Laptev Sea is different, which is associated with different water salinity in these water areas.

3. CONCLUSION

The study utilizes a two-stage equivalent imaging optical system of a digital holographic camera: optical imaging at the stage of digital hologram recording and fully virtual, calculated reconstruction of images. Such an equivalent scheme allowed constructing a mathematical model for an in-line scheme that establishes a one-to-one correspondence between dimensional and spatial parameters of the digital holographic image and the holographing object. The calibration makes it possible to find the values of model constants to determine the real size and longitudinal coordinate of the object using its holographic image.

The paper shows that the optimal number of calibration experiments (or calibers used with simultaneous registration per one hologram) is 4. This does not require data on the optical properties of the components and media (in this case, water, glass and air) included in the equivalent optical scheme. Besides, the difference in the curvature of the wave fronts of recording and reconstruction waves is automatically taken into account.

The in situ experiments showed that for the developed mathematical model one calibration is quite sufficient within the same water area, since the values of coefficients change slightly. Moreover, by changing the calibration coefficients, we may face the change in the optical properties of the medium in which the measurements are taken.

ACKNOWLEDGEMENTS

The in situ studies using a digital holographic camera were carried out with the financial support of the Russian Science Foundation (grant No. 20-17-00185).

The analysis of the optical properties of a digital holographic camera was funded by the Russian Foundation for Basic Research (project No. 19-32-90233).

REFERENCES

[1] Dyomin, V., Gribenyukov, A., Davydova, A., Zinoviev, M., Olshukov, A., Podzyvalov, S., Polovtsev, I. and Yudin, N., "Holography of particles for diagnostics tasks [Invited]," Appl. Opt. **58**(34), G300 (2019).

[2] Giering, S. L. C., Cavan, E. L., Basedow, S. L., Briggs, N., Burd, A. B., Darroch, L. J., Guidi, L., Irisson, J.-O., Iversen, M. H., Kiko, R., Lindsay, D., Marcolin, C. R., McDonnell, A. M. P., Möller, K. O., Passow, U., Thomalla, S., Trull, T. W. and Waite, A. M., "Sinking Organic Particles in the Ocean—Flux Estimates from in situ Optical Devices," Front. Mar. Sci. **6**(February), 834 (2020).

[3] Walcutt, N. L., Knörlein, B., Cetinić, I., Ljubesic, Z., Bosak, S., Sgouros, T., Montalbano, A. L., Neeley, A., Menden-Deuer, S. and Omand, M. M., "Assessment of holographic microscopy for quantifying marine particle size and concentration," Limnol. Oceanogr. Methods **18**(9), 516–530 (2020).

[4] Memmolo, P., Carcagnì, P., Bianco, V., Merola, F., Goncalves da Silva Junior, A., Garcia Goncalves, L. M., Ferraro, P. and Distante, C., "Learning Diatoms Classification from a Dry Test Slide by Holographic Microscopy," Sensors (Basel). **20**(21), 1–13 (2020).
[5] Malkiel, E., Sheng, J., Katz, J., and Strickler, J. R., "The three-dimensional flow field generated by a feeding calanoid copepod measured using digital holography," J. Exp. Biol. **206**, 3657–3666 (2003).
[6] Hobson, P. R., and Watson, J., "The principles and practice of holographic recording of plankton," J. Opt. A 4, S34–S49 (2002).
[7] Katz, J. and Sheng, J., "Applications of Holography in Fluid Mechanics and Particle Dynamics," Annu. Rev. Fluid Mech. **42**(1), 531–555 (2009).
[8] Graham, G. W. and Nimmo Smith, W. A. M., "The application of holography to the analysis of size and settling velocity of suspended cohesive sediments," Limnol. Oceanogr. Methods **8**(1), 1–15 (2010).
[9] Zhu, Y., Hang Yeung, C. and Lam, E. Y., "Digital holographic imaging and classification of microplastics using deep transfer learning," Appl. Opt. **60**(4), A38 (2021).
[10] Bianco, V., Memmolo, P., Carcagnì, P., Merola, F., Paturzo, M., Distante, C. and Ferraro, P., "Microplastic Identification via Holographic Imaging and Machine Learning," Adv. Intell. Syst. **2**(2), 1900153 (2020).
[11] Talapatra, S., Sullivan, J., Katz, J., Twardowski, M., Czerski, H., Donaghay, P., Hong, J., Rines, J., McFarland, M., Nayak, A. R. and Zhang, C., "Application of in-situ digital holography in the study of particles, organisms and bubbles within their natural environment," Proc. SPIE - Int. Soc. Opt. Eng. **8372**, W. W. Hou and R. Arnone, Eds., 837205 (2012).
[12] Shao, S., Li, C. and Hong, J., "A hybrid image processing method for measuring 3D bubble distribution using digital inline holography," Chem. Eng. Sci.(July) (2019).
[13] Wu, Y., Zhang, H., Wu, X. and Cen, K., "Quantifying bubble size and 3D velocity in a vortex with digital holographic particle tracking velocimetry (DHPTV)," Flow Meas. Instrum. **76**, 101826 (2020).
[14] Kemppinen, O., Laning, J. C., Mersmann, R. D., Videen, G. and Berg, M. J., "Imaging atmospheric aerosol particles from a UAV with digital holography," Sci. Rep. **10**(1), 1–12 (2020).
[15] Fugal, J. P., and Shaw, R. A., "Cloud particle size distributions measured with an airborne digital in-line holographic instrument," Atmos. Meas. Technol. **2**, 259–271 (2009).
[16] Wu, Y.-C., Shiledar, A., Li, Y.-C., Wong, J., Feng, S., Chen, X., Chen, C., Jin, K., Janamian, S., Yang, Z., Ballard, Z. S., Göröcs, Z., Feizi, A. and Ozcan, A., "Air quality monitoring using mobile microscopy and machine learning," Light Sci. Appl. **6**(9), e17046–e17046 (2017).
[17] Beals, M. J., Fugal, J. P., Shaw, R. A., Lu, J., Spuler, S. M. and Stith, J. L., "Holographic measurements of inhomogeneous cloud mixing at the centimeter scale," Science. **350**(6256), 87–90 (2015).
[18] Dyomin, V. V., Gribenyukov, A. I., Davydova, A. Y., Olshukov, A. S., Polovtsev, I. G., Podzyvalov, S. N., Yudin, N. N. and Zinovev, M. M., "Visualization of volumetric defects and dynamic processes in crystals by digital IR holography," HTh3H.3 (2020).
[19] U. Schnars and W. P. O. Juptner, "Digital recording and numerical reconstruction of holograms," Meas. Sci. Technol. 13, R85–R101 (2002).
[20] Collier, R. J., Burckhardt, C. B. and Lin, L. H., [Optical Holography], 1st edition, Academic Press, New York (1971).
[21] Poon, T-C., and Liu, J-P., [Introduction to modern digital holography: with MATLAB], Cambridge University Press, New York (2014).
[22] Schnars, U., and Jueptner, W., [Digital Hologram Recording, Numerical Reconstruction, and Related Techniques], Springer, (2005).
[23] Yaroslavsky, L., [Digital Holography and Digital Image Processing Principles, Methods, Algorithms] Academic, (2004).
[24] Dyomin, V. V., Olshukov, A. S. and Kamenev, D. V., "Evaluation of the plankton species coordinates from digital holographic video," Ocean. 2011 IEEE - Spain, 1–6 (2011).
[25] Dyomin, V. V., Davydova, A. Y., Morgalev, S. N., Kirillov, N. S., Olshukov, A., Polovtsev, I. and Davydov, S., "Monitoring of Plankton Spatial and Temporal Characteristics with the Use of a Submersible Digital Holographic Camera," Front. Mar. Sci. **7**(653), 1–9 (2020).
[26] Hecht, E., "Optics 2nd edition," Addison-Wesley Publ. Co. (1987).
[27] Zimmer, H.G., "Geometrical Optics," New York: Springer-Verlag (1970).
[28] Pedrotti, F.L., Pedrotti, L.S., & Pedrotti, L.M., "Introduction to Optics (3rd ed.)," Cambridge: Cambridge University Press. (2017)

[29] Malacara, D. and Malacara, Z., [Handbook of Optical Design, Second Edition], Marcel Dekker, Inc., New York (2004).
[30] Levenberg, K., "A method for the solution of certain non-linear problems in least squares," Q. Appl. Math. **2**(2), 164–168 (1944).
[31] Marquardt, D. W., "An Algorithm for Least-Squares Estimation of Nonlinear Parameters," J. Soc. Ind. Appl. Math. **11**(2), 431–441 (1963).